

Journal Pre-proof

Tricyclic heterocycles display diverse sensitivity to the A147T TSPO polymorphism

Renee Sokias, Eryn L. Werry, Hei Wun Alison Cheng, James H. Lloyd, Greta Sohler, Jonathan J. Danon, Andrew P. Montgomery, Jonathan J. Du, Quanqing Gao, David E. Hibbs, Lars M. Ittner, Tristan A. Reekie, Michael Kassiou



PII: S0223-5234(20)30697-8

DOI: <https://doi.org/10.1016/j.ejmech.2020.112725>

Reference: EJMECH 112725

To appear in: *European Journal of Medicinal Chemistry*

Received Date: 29 June 2020

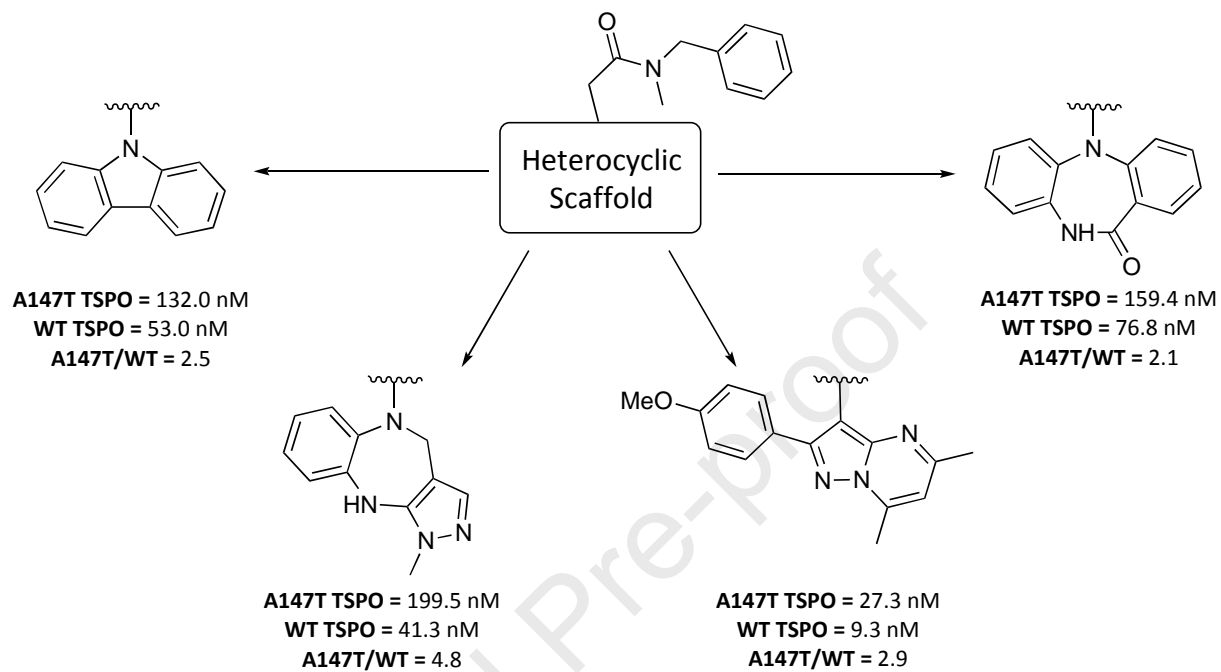
Revised Date: 2 August 2020

Accepted Date: 3 August 2020

Please cite this article as: R. Sokias, E.L. Werry, H.W. Alison Cheng, J.H. Lloyd, G. Sohler, J.J. Danon, A.P. Montgomery, J.J. Du, Q. Gao, D.E. Hibbs, L.M. Ittner, T.A. Reekie, M. Kassiou, Tricyclic heterocycles display diverse sensitivity to the A147T TSPO polymorphism, *European Journal of Medicinal Chemistry*, <https://doi.org/10.1016/j.ejmech.2020.112725>.

This is a PDF file of an article that has undergone enhancements after acceptance, such as the addition of a cover page and metadata, and formatting for readability, but it is not yet the definitive version of record. This version will undergo additional copyediting, typesetting and review before it is published in its final form, but we are providing this version to give early visibility of the article. Please note that, during the production process, errors may be discovered which could affect the content, and all legal disclaimers that apply to the journal pertain.

© 2020 Elsevier Masson SAS. All rights reserved.



Tricyclic heterocycles display diverse sensitivity to the A147T TSPO polymorphism

Renee Sokias,^{#§} Eryn L. Werry,^{#§} Hei Wun Alison Cheng,[◇] James H. Lloyd,[#] Greta Sohler,[#] Jonathan J. Danon,[#] Andrew P. Montgomery,[#] Jonathan J. Du,[△] Quanqing Gao,[△] David E. Hibbs,[△] Lars M. Ittner,[◇] Tristan A. Reekie[#] and Michael Kassiou.^{#*}

[#]School of Chemistry, Faculty of Science and [◇]School of Medical Sciences, Faculty of Medicine and Health, [△]Sydney School of Pharmacy, Faculty of Medicine and Health, The University of Sydney, NSW, Australia, 2006 [◇]Department of Biomedical Sciences, Faculty of Medicine and Health Sciences, 2 Technology Place, Macquarie University, NSW, Australia, 2109

Abstract

The 18 kDa translocator protein (TSPO) is a target for the development of imaging agents to detect neuroinflammation. The clinical utility of second-generation TSPO ligands has been hindered by the presence of a polymorphism, *rs6971*, which causes a non-conservative substitution of alanine for threonine at amino acid residue 147 (TSPO A147T). Given the complex nature of TSPO binding, and the lack of non-discriminating high-affinity ligands at both wild type and A147T forms of TSPO, a series of novel TSPO ligands containing various heterocyclic scaffolds was developed to explore the pharmacophoric drivers of affinity loss at TSPO A147T. In general, *N*-benzyl-*N*-methyl-substituted amide ligands showed increased affinity at TSPO A147T, and a pyrazolopyrimidine acetamide containing this motif displayed low nanomolar binding affinities to both TSPO forms.

Keywords

TSPO, microglia, polymorphism, docking, non-discriminating, structure-activity relationships.

Introduction

The 18 kDa translocator protein (TSPO) is a five transmembrane domain protein expressed ubiquitously throughout the body.¹ TSPO expression is predominant in steroid-synthesising tissues within the periphery.^{2, 3} Minimal TSPO expression occurs in the non-pathological central nervous system (CNS),³ but expression is upregulated in activated glia in areas damaged by neurodegenerative diseases.^{1, 3} Molecular imaging using TSPO positron emission tomography (PET) ligands can image areas affected by neuroinflammation in preclinical and clinical studies of neurodegenerative diseases.⁴ Furthermore, the upregulation of the TSPO within cancerous cells has attracted considerable attention as a potential biomarker for neoplastic growth or as a novel protein target for chemotherapy.^{5, 6}

Development of TSPO ligands has been hindered by a single nucleotide polymorphism (SNP; rs6971) in the TSPO that results in the replacement of an alanine (Ala; A) with a threonine (Thr; T) at amino acid residue 147 (A147T).^{7, 8} Second-generation TSPO PET ligands such as DPA-713, XBD-173 and PBR-28 show three distinct binding patterns to tissue from human donors: high-, mixed-, and low-affinity binding. The most common TSPO form, Ala/Ala, is associated with a high-affinity binding phenotype, Ala/Thr leads to mixed-affinity binding, while Thr/Thr displays low-affinity binding.^{7, 8} The TSPO protein's conformational change resulting from this amino acid substitution significantly influences binding of second-generation TSPO ligands.⁷⁻¹⁰ The presence of the differing binding affinities, particularly in patients who are low-affinity binders, complicates the quantitative assessment of PET data using second-generation ligands. TSPO PET images of low-affinity binders have a significantly lower signal-to-noise ratio, and the clinical usefulness of this approach is therefore limited in these patients.¹¹ The first-generation ligand PK-11195 (**1**) does not show loss of affinity at A147T TSPO, however its clinical use is complicated by high non-specific binding, high plasma protein binding and low blood-brain barrier permeability.¹² The closely related 4-azaisostere (**2**) did not show loss in affinity at A147T TSPO in membranes prepared from human tissue,¹⁰ but a three-fold reduction in PET binding potential in low-affinity binders compared to high-affinity binders.¹³ Given this, a TSPO PET ligand that binds with an equally high-affinity to both A147T and wild type TSPO *in vivo* is currently elusive.

Discovery of new ligands with improved binding profiles would be facilitated by an understanding of pharmacophoric features that influence discrimination between wild type and A147T TSPO. In reported structure-activity relationship (SAR) studies, pendant acetamide moieties were demonstrated to be key structural requirements for wild type TSPO affinity across various ligand classes.¹⁴ Moreover, the optimum binding affinity to wild type TSPO required two lipophilic substituents on the terminal acetamide.^{14, 15} Although aliphatic substituents on the terminal acetamide are widely reported, recent SAR studies demonstrated that a *N*-benzyl substituent is crucial for enhancing wild type TSPO affinity.^{15, 16}

Additionally, given that numerous ligand classes can bind the TSPO, efforts have also been directed toward determining whether the heterocyclic scaffold interacts with the binding sites present on both TSPO isoforms. Scaffolds including carbazoles (**3**), pyrazolopyrimidines (**4**), pyrazolobenzodiazepines (**5**), and dibenzodiazepines (**6**) were explored, based on their reported bioactivity, high affinity, bioavailability, and their synthetic accessibility.¹⁷⁻¹⁹

The work herein explores the effect of the heterocyclic scaffold on TSPO binding, while simultaneously exploring the effect of the acetamide substituents. We report that for ligands which bind to TSPO, discrimination at A147T TSPO can be reduced by inclusion of an *N*-benzyl-*N*-methyl substitution on the acetamide motif in most cases.

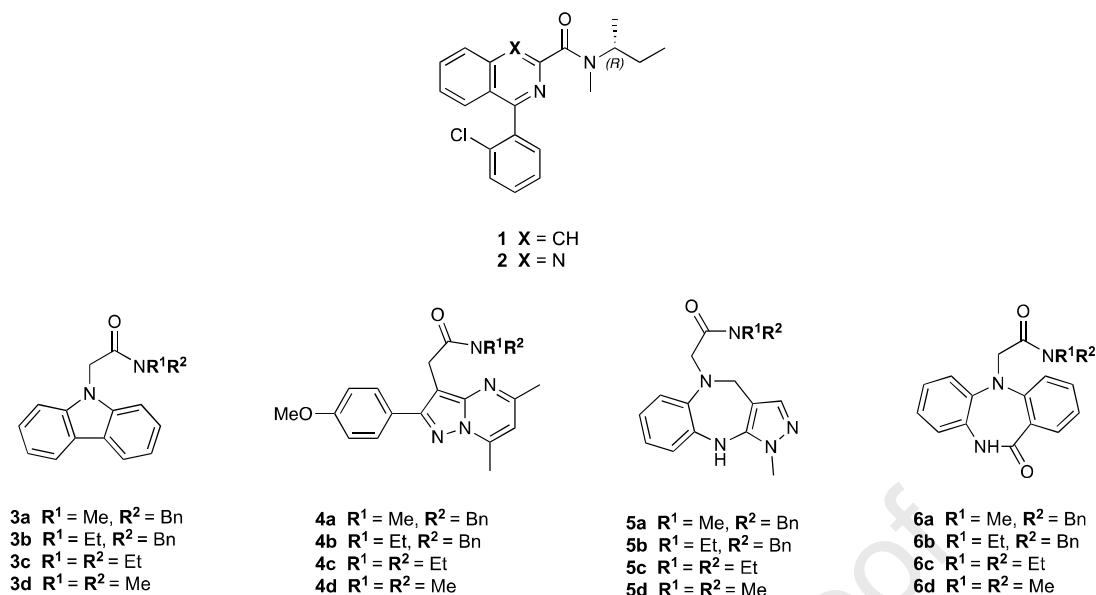
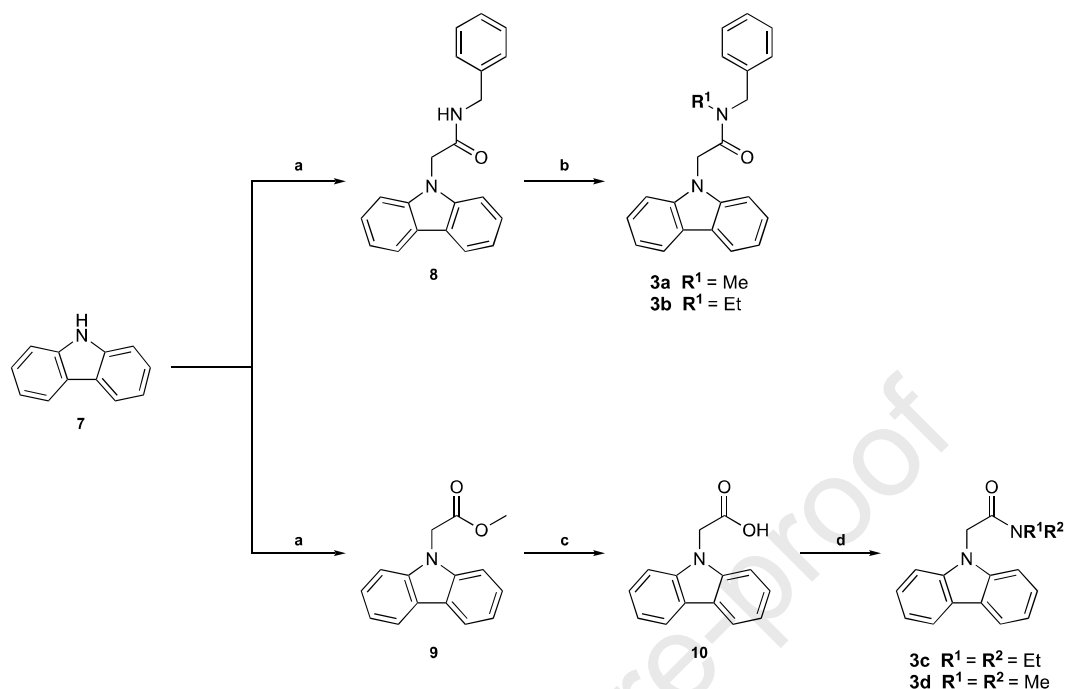


Figure 1: Previously reported TSPO ligands **1–2**,¹⁰ **3**²⁰ and novel TSPO ligands **4–6**.

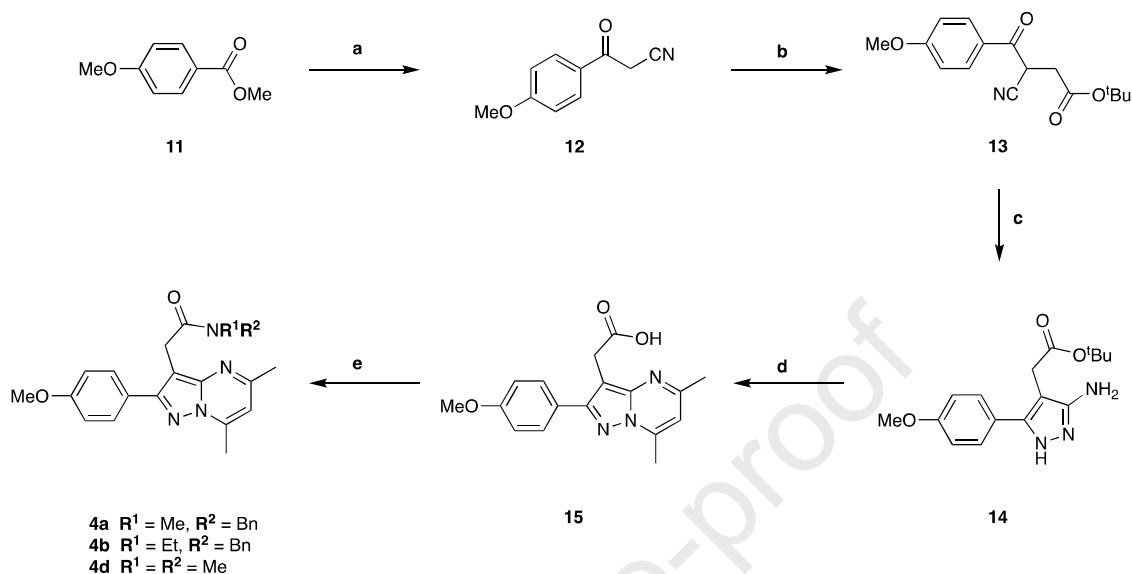
Results and Discussion

Chemistry. Carbazole acetamide ligands **3a–3d** have been previously reported²⁰ and were synthesised according to Scheme 1. Initial *N*-alkylation of 9*H*-carbazole (**7**) with the appropriate alkylating agent (*N*-benzyl-2-bromoacetamide or ethyl bromoacetate), in the presence of sodium hydride afforded intermediates **8** and **9** in excellent yields (81–86%). Subsequent *N*-methylation or *N*-ethylation of **8** with methyl or ethyl iodide, in the presence of potassium *tert*-butoxide, furnished target ligands **3a** and **3b** in excellent yields (87–90%). Hydrolysis of methyl ester **9**, under basic conditions, afforded carboxylic acid **10** in good yield (72%). HBTU-mediated coupling of **10** with diethylamine or dimethylamine furnished ligands **3c** and **3d** in good yields (76–83%). *N*-benzyl-2-bromoacetamide was synthesised from benzylamine and 2-bromoacetyl bromide (see Experimental section).

Scheme 1. Synthetic route for the carbazole acetamide ligands.^a

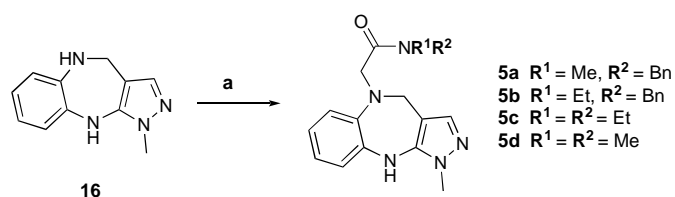
^aReagents and Conditions: a) i) THF, NaH, 0 °C, 30 min; ii) *N*-benzyl-2-bromoacetamide or ethyl bromoacetate, 0 °C–rt, 2 h, 81–86%; b) KOtBu, appropriate iodoalkane, THF, 0 °C–rt, 17 h, 87–90%; c) LiOH, THF/H₂O, Δ, 4 h, 72%; d) HBTU, DIPEA, dimethylamine, DMF, rt, 16 h, 83%.

Pyrazolopyrimidine acetamide ligands **4a–4d** were synthesised according to Scheme 2, while synthesis of ligand **4c** was previously reported.²¹ Commercially available methyl *p*-anisate (**11**) was treated with sodium methoxide, followed by acetonitrile to generate cyanoacetophenone **12**. Deprotonation of **12** to the corresponding enolate, followed by treatment with *tert*-butyl 2-bromoacetate, gave compound **13**. Condensation of compound **13** with hydrazine monohydrate afforded the aminopyrazole **14**. Further condensation of aminopyrazole **14** with acetylacetone, followed by basic hydrolysis of the *tert*-butyl ester furnished the pyrazolopyrimidine core **15**. Amide coupling with the appropriate secondary amine furnished the desired pyrazolopyrimidine acetamide ligands **4a–4d**.

Scheme 2. Synthetic route for the pyrazolopyrimidine acetamide ligands.^a

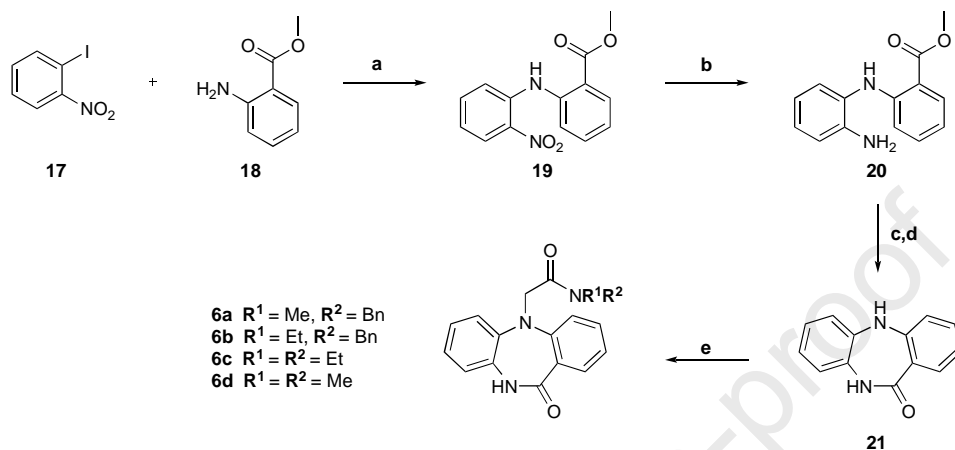
^aReagents and Conditions: a) MeCN, NaOMe, PhMe, Δ , 18 h, 44%; b) NaOH, *tert*-butyl 2-bromoacetate, EtOH, rt, 24 h, 57%; c) NH₂NH₂·H₂O, cat. AcOH, EtOH, Δ , 13 h, 49%; d) i) Acetylacetone, EtOH, Δ , 5 h; ii) NaOH, EtOH, Δ , 12 h, 92% (over 2 steps); e) PyBOP, DIPEA, NHR¹R², DMF, 55–86%.

The pyrazolobenzodiazepine acetamide ligands were synthesised from **16**,²² according to Scheme 3. Compound **16** was *N*-alkylated with the appropriate alkylating agent in the presence of triethylamine and furnished target pyrazolobenzodiazepine acetamide ligands **5a–5d**.

Scheme 3. Synthesis of the pyrazolobenzodiazepine acetamide ligands.^a

^aReagents and Conditions: a) Et₃N, THF, appropriate alkylating agent, rt, 19 h, 76–81%.

The dibenzodiazepine acetamide ligands were synthesised according to Scheme 4. The synthesis of key dibenzodiazepine intermediate **21** was achieved by first preparing intermediate **19** *via* a palladium-catalysed Buchwald-Hartwig cross-coupling reaction. Subsequent catalytic hydrogenation with palladium on carbon (Pd/C) afforded intermediate **20**. Base-mediated hydrolysis of the methyl ester to the carboxylic acid followed by amide coupling furnished the desired dibenzodiazepine intermediate **21**. Dibenzodiazepine acetamide ligands **6a–6d** were obtained by *N*-alkylation of **21** with the appropriate alkylating agent in the presence of potassium *tert*-butoxide.

Scheme 4. Synthetic route for the dibenzodiazepine acetamide ligands.^a

^aReagents and Conditions: a) $\text{Pd}(\text{OAc})_2$, BINAP, Cs_2CO_3 , PhMe, 90 °C, 17 h, 77%; b) Pd/C (10% w/w), EtOAc, H_2 (1 atm), rt, 6 h, 92%; c) LiOH, MeOH/ H_2O , Δ , 6 h; d) HBTU, DIPEA, DMF, 10 min, 82% (over 2 steps); e) KOTBu, appropriate alkylating agent, THF, 0 °C–rt, 18 h, 83–87%.

Assessment of TPSO binding affinity. The previously reported carbazole acetamide series of ligands (**3a–d**) provide an important comparison and are discussed here briefly.²⁰ Ligand **3a**, featuring a methyl and benzyl group at the R^1 and R^2 positions displayed moderate binding to both TSPO isoforms (132.0 nM and 53.0 nM for A147T and WT, respectively). Substituting the methyl group at the R^1 position with an ethyl group (**3b**) decreased binding at both isoforms (459.6 nM and 91.6 nM for A147T and WT, respectively). Ligand **3c**, with ethyl substituents at the R^1 and R^2 position increased binding at the TSPO wild type (30.1 nM) and showed moderate binding affinity at the TSPO A147T (176.6 nM). Binding affinity was completely nullified at both TSPO isoforms for ligand **3d**, which features methyl substituents at both R^1 and R^2 positions. Examining the A147T-to-wild type ratio shows that the carbazole acetamide series showed discrimination to both TSPO isoforms, although the degree of discrimination was smallest with the *N*-benzyl-*N*-methyl substituent.

The second series of ligands (**4a–4d**) contained a pyrazolopyrimidine scaffold and examined the same modifications at the R^1 and R^2 positions. Ligand **4a**, which featured a methyl substituent at the R^1 position and a benzyl group at the R^2 position, displayed strong binding at both TSPO isoforms (27.3 nM and 9.3 nM for A147T and WT, respectively). Substituting the R^1 group with an ethyl group (**4b**) selectively decreased binding at the A147T TSPO isoform (80.6 nM) without impacting affinity at wild type TSPO. Ligand **4c**, featuring an ethyl substituent at both the R^1 and R^2 , displayed decreased binding at both isoforms (98.8 nM and 19.5 nM for A147T and WT, respectively), compared to the benzyl-substituted analogues (**4a**, **4b**). Binding affinity dropped off greatly with incorporation of an *N,N*-dimethyl substituent (**4d**) into the pyrazolopyrimidine scaffold. The pyrazolopyrimidine acetamide series again showed discrimination between TSPO isoforms.

The third series of ligands (**5a–5d**) contained a pyrazolobenzodiazepine scaffold and modifications at the R^1 and R^2 positions. Ligand **5a**, which featured a methyl and benzyl substituent at the R^1 and R^2 positions displayed the strongest, or equal strongest, binding affinity at both TSPO isoforms (199.5 nM and 41.3 nM for A147T and WT, respectively) within the pyrazolobenzodiazepine

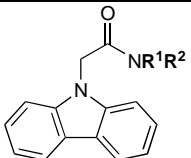
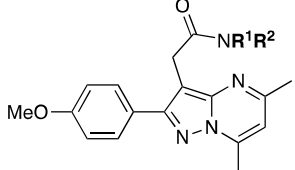
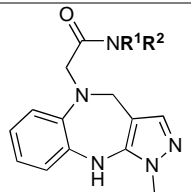
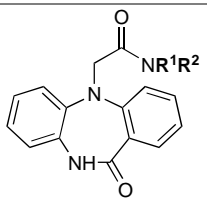
series, although TSPO isoform discrimination was still observed. Incorporation of an *N*-benzyl-*N*-ethyl R¹R² group into the scaffold (**5b**) had little impact on affinity compared to **5a**, but substituting the R¹R² group with an *N,N*-diethyl group (**5c**) decreased binding at both TSPO isoforms. Replacement of the R¹R² group with an *N,N*-dimethyl group (**5d**) abolished binding at both isoforms.

The fourth series of ligands (**6a–6d**) contained a dibenzodiazepinone scaffold and modifications at the R¹ and R² positions. The best in this series, ligand **6b**, featured an ethyl substituent at the R¹ and a benzyl group at the R² position, displayed moderate binding affinity at A147T TSPO (99.4 nM) and strong binding to the wild type TSPO (15.8 nM). A comparison between ligands **6a–6c** showed that by substituting the R¹ group with a methyl group (**6a**) or R² group with an ethyl group (**6c**) decreased binding at both TSPO isoforms. This observation differed from the pyrazolobenzodiazepine series (**5**), where the *N*-benzyl-*N*-methyl substituted acetamide was more favourable over the *N*-benzyl-*N*-ethyl. However, ligand **6a** still displayed moderate binding affinities to both TSPO isoforms (159.4 nM and 76.8 nM for A147T and WT, respectively), and displayed the least discrimination between the two TSPO forms throughout the dibenzodiazepinone series.

Drawing all this together, two trends regarding the influence of the R¹R² group within each scaffold series appear. Firstly, with the exception of the pyrazolobenzodiazepine scaffold, decoration with an *N*-benzyl-*N*-methyl R¹R² group imparts the least discrimination between TSPO WT and A147T. Secondly, incorporation of an *N,N*-dimethyl group imparts poor binding at both forms of TSPO (**3–6d**). The binding pocket that the R¹R² groups access in TSPO is lipophilic²³ so it is possible that the more lipophilic R¹R² groups in the **a–c** analogues within each scaffold form stronger interactions with the binding pocket than those of the **d** analogues. These results are congruent with previous studies that hypothesize the necessity of a fully occupied lipophilic pocket with a bulky *N*-alkyl group for greater TSPO affinity.²⁴

Drawing trends across scaffolds was more complex. Comparing each R¹,R² substitution across scaffolds revealed that the pyrazolopyrimidine scaffold afforded the highest affinity at each isoform of TSPO. However, the complex nature of the heterocycle on binding was revealed by comparing ligands **3a–c** and **5a–c**. For *N*-benzyl-*N*-methyl derivatives (**3a** vs **5a**), the pyrazolobenzodiazepine scaffold was more favourable at the wild type and less favourable at the A147T TSPO isoform, compared to the carbazole scaffold. In contrast, the pyrazolobenzodiazepine scaffold was more favourable at both forms of TSPO in *N*-benzyl-*N*-ethyl-substituted derivatives (**3b** vs **5b**), and was less favourable at both TSPO isoforms in *N,N*-diethyl-substituted derivatives (**3c** vs **5c**). This suggests that the influence of the heterocycle on affinity is dependent on the identity of the R¹ and R² substituents.

Table 1. TSPO binding affinities (K_i) using membranes from TSPO wild type and A147T over-expressing HEK-293T cells. Values represent the mean \pm SEM from at least three independent experiments performed in duplicate.

	N	R ¹	R ²	K _i (nM)		A147T: Wild Type
				A147T	Wild Type	
	3a	Me	Bn	132.0 \pm 8.0	53.0 \pm 7.0	2.5
	3b	Et	Bn	459.6 \pm 83.0	91.6 \pm 1.0	5.0
	3c	Et	Et	176.6 \pm 41.6	30.1 \pm 3.6	5.9
	3d	Me	Me	>10 000	>10 000	N/A
	4a	Me	Bn	27.3 \pm 3.6	9.3 \pm 2.3	2.9
	4b	Et	Bn	80.6 \pm 4.3	6.2 \pm 1.0	13.0
	4c	Et	Et	98.8 \pm 2.3	19.5 \pm 3.5	5.1
	4d	Me	Me	559.8 \pm 59.3	337.9 \pm 29.1	1.7
	5a	Me	Bn	199.5 \pm 10.5	41.3 \pm 8.1	4.8
	5b	Et	Bn	226.9 \pm 30.7	41.3 \pm 8.6	5.5
	5c	Et	Et	2256.6 \pm 335.6	493.0 \pm 45.2	4.6
	5d	Me	Me	>10 000	>10 000	N/A
	6a	Me	Bn	159.4 \pm 17.6	76.8 \pm 16.2	2.1
	6b	Et	Bn	99.4 \pm 9.8	15.8 \pm 1.3	6.2
	6c	Et	Et	2357.8 \pm 412.4	200.5 \pm 29.8	11.8
	6d	Me	Me	>10 000	>10 000	N/A

Docking Studies. Docking studies were used to examine how each heterocyclic scaffold binds to both WT and A147T TSPO. As the *N*-benzyl-*N*-methyl series, in general, showed the least discrimination between A147T and wild type TSPO, ligands **3a**, **4a**, **5a** and **6a** were chosen for docking studies. Docking and MM-GBSA Δ G binding scores (obtained by combining molecular mechanics (MM) terms with a generalised Born and surface area (MM-GBSA) solvent model)²⁵ are summarised in Table 2.

Table 2. Docking and MM-GBSA ΔG binding scores and key interacting residues for ligands docked into the chosen receptors *via* extra precision (XP) docking. Residues in blue interact with the ligand only in the wild type model and residues in green interact with the ligand only in the A147T model.

Ligand	docking score ^a (kcal/mol)		MMGBSA ΔG Bind ^b (kcal/mol)		Interacting residues ^c
	A147T	WT	A147T	WT	
3a	-9.602	-9.706	-75.43	-67.37	Trp53, Trp95, Phe99, Trp143, Arg24
4a	-5.248	-7.668	-85.77	-71.98	Arg24, Tyr34, Trp53, Trp95, Phe100, Trp143
5a	-9.541	-9.479	-74.44	-92.64	Tyr34, Trp53, Trp143, Arg24, Trp95
6a	-12.885	-9.601	-81.22	-77.24	Ser23, Phe99, Arg24, Trp53, Tyr57, Asn92, Trp95, Trp143

^aDocking scores obtained from extra precision Glide docking are an estimate of protein-ligand binding energies. More negative scores indicate more favourable binding interactions

^bMM-GBSA binding energies are approximate free energies of binding. More negative scores indicate more favourable binding interactions.

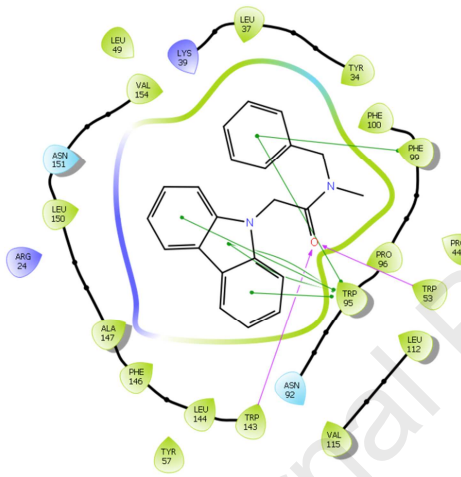
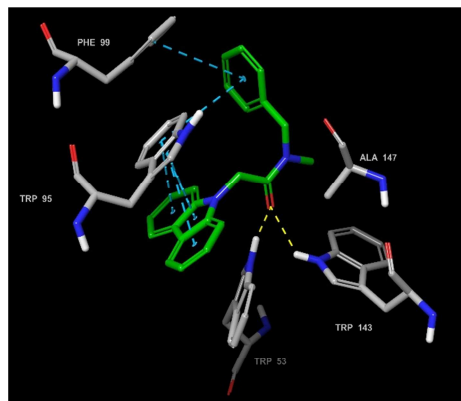
^cKey interactions residues are taken from the 2D ligand interaction function of Maestro v12.1.

Ligands **3a** and **5a** had similar docking scores for both WT and A147T TSPO, while a difference of ~ 2.5 kcal/mol and ~ 3.3 kcal/mol were observed for ligands **4a** and **6a** respectively. For both **4a** and **6a** the binding conformation observed was similar in both WT and A147T TSPO. The differences in the docking scores for both ligands can be attributed to the pyrazolopyrimidine and dibenzodiazepine scaffolds being slightly distorted in A147T TSPO by Thr147 when compared to the WT. The MM-GBSA binding scores were similar for each ligand between the WT and A147T TSPO.

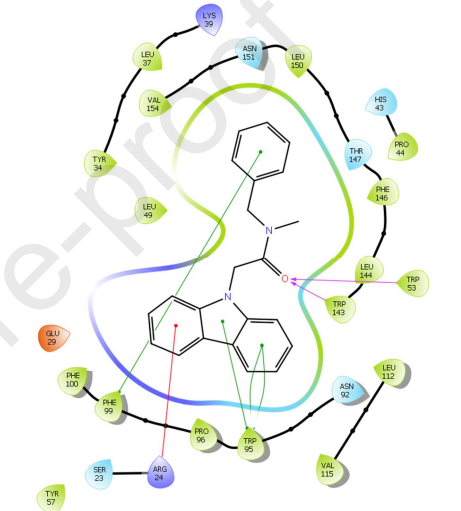
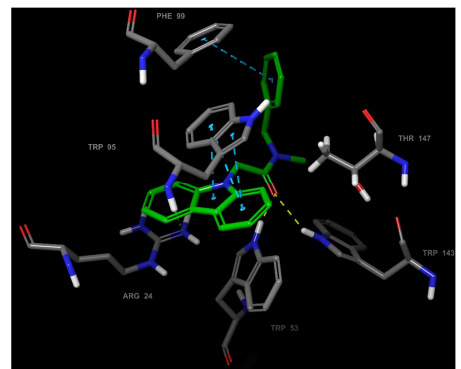
Binding poses for each ligand are shown in Figure 2. Each ligand exhibited binding poses where π - π interactions are observed with Trp53 and Trp95 in both WT and A147T TSPO (**5a** WT being the only exception). This network of π - π interactions with the heterocyclic scaffolds appears to be crucial in orienting the ligands within the predicted binding site. In addition, hydrogen bond interactions of the acetamide oxygen of each ligand with the indolic NH of Trp143 and Trp153 was also conserved in both WT and A147T TSPO. The lower K_i observed for the pyrazolopyrimidine scaffold **4a** in comparison to the other heterocyclic scaffolds can be rationalised by the additional π - π interactions observed in both the WT and A147T TSPO. This interaction is between Phe100 and the 4-methoxyphenyl group at the 2-position of pyrazolopyrimidine scaffold.

3a

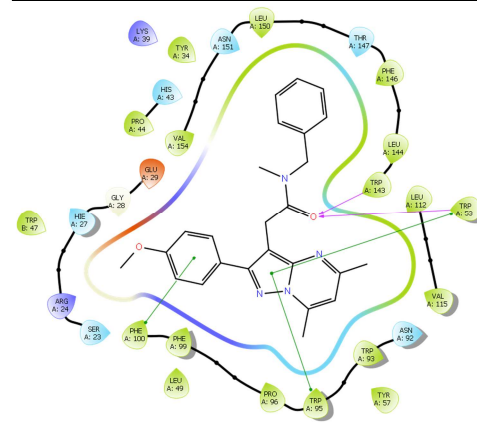
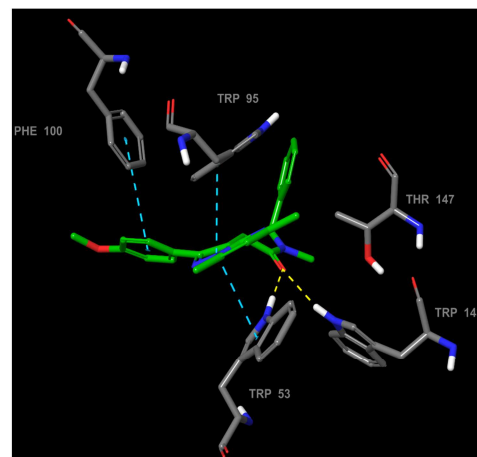
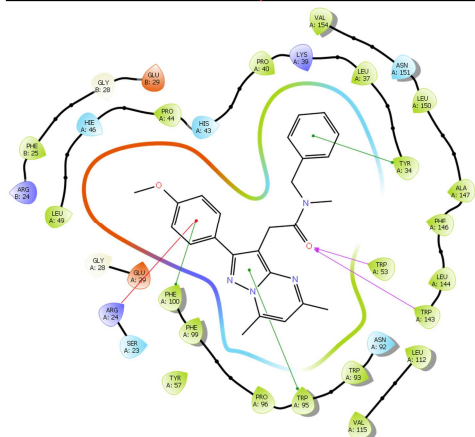
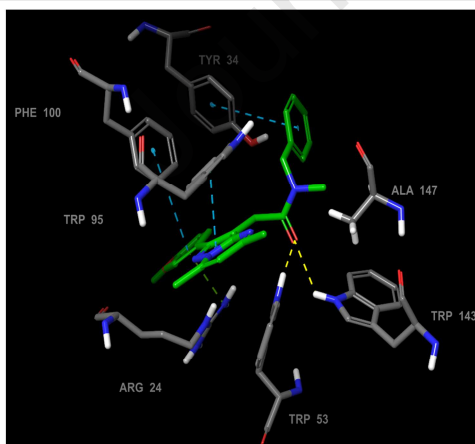
WT TSPO



A147T TSPO

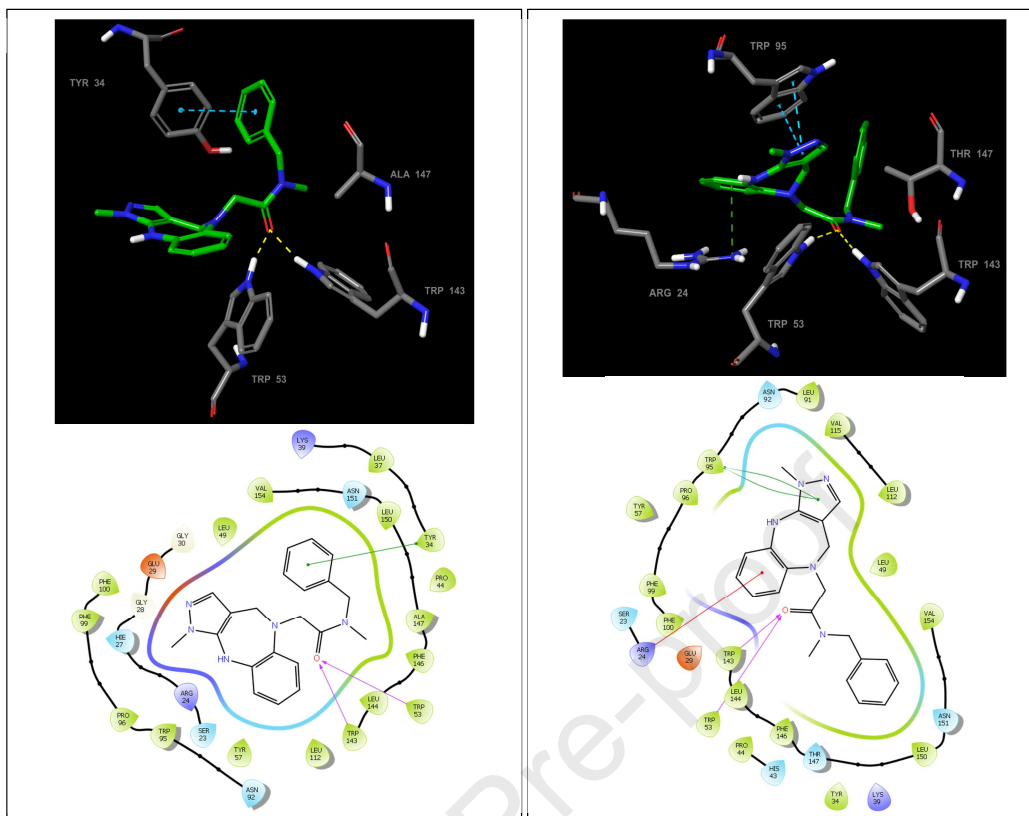


4a



Journal Pre-proof

5a



6a

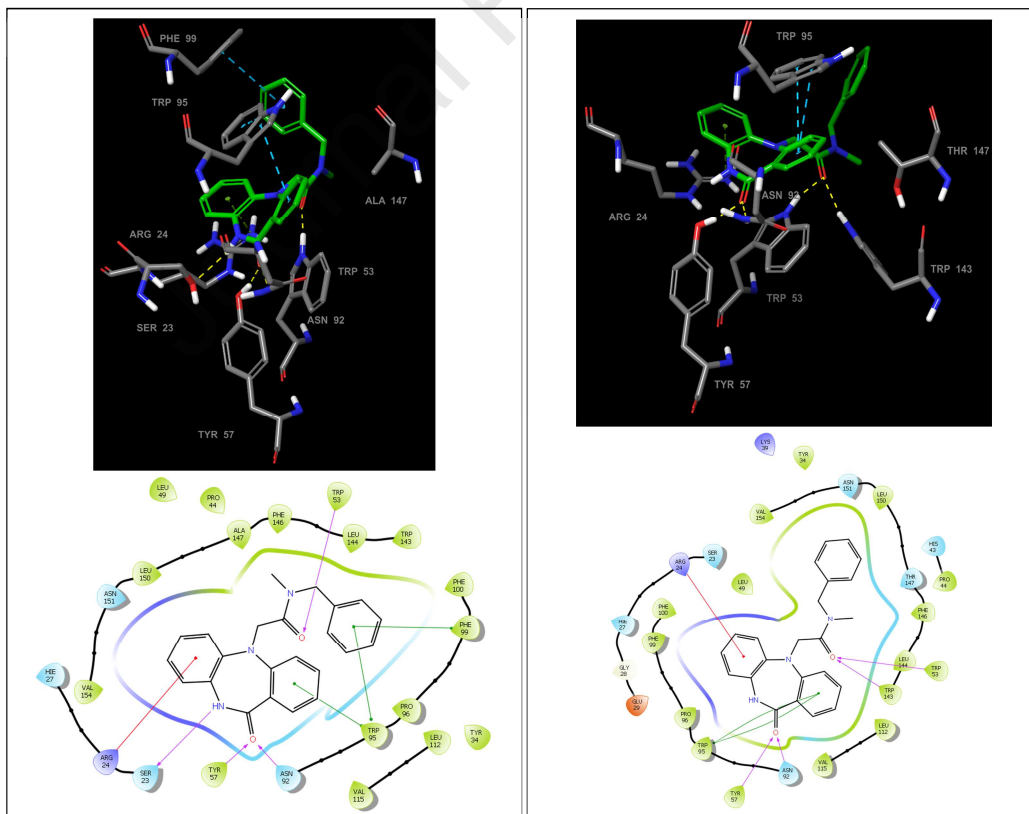


Figure 2. 3D and 2D ligand binding depictions of TSPO ligands **3a**, **4a**, **5a** and **6a** into the chosen receptors. Purple lines represent hydrogen bonding, green lines represent π - π stacking and red lines represent π -cation bonds. The crystal structure of TSPO protein from *Bacillus Cereus* (PDB ID: 4RYI), was used as the template for homology modelling.

Conclusion

Taken together, these findings highlight the effect the heterocyclic scaffold has on the binding affinity at both TSPO isoforms. The pyrazolopyrimidine scaffold (**4**) remains a promising scaffold for TSPO ligands. Although lipophilic bulk on *N,N*-disubstituted acetamide heterocyclic scaffolds is essential to ensure binding to wild type and A147T TSPO, lowered discrimination at A147T TSPO is predominantly seen with *N*-benzyl-*N*-methyl ligands, compared to *N,N*-diethyl and *N*-benzyl-*N*-ethyl ligands. This knowledge can be used to inform further development of TSPO ligands with equally high-affinity at both the TSPO wild type and A147T for use in diagnosis and treatment of neurodegenerative disorders and several cancer types.

Experimental section

General Experimental

Unless otherwise stated, all solvents and reagents were purchased from commercial sources and used without further purification. All reagents were weighed out under ambient conditions. All reactions were performed under nitrogen or argon. Nuclear magnetic resonance spectra were recorded on Bruker Advance DRX 300, 400 or 500 Ascend spectrometers at 300, 400 or 500 MHz ¹H NMR frequency, 75, 101 or 151 MHz ¹³C NMR frequency and 282 MHz ¹⁹F NMR frequency. The NMR spectra for several target compounds showed the presence of rotamers as a result of the amide functionality. For the sake of simplicity, the NMR signals for only one rotamer are reported. Low-resolution mass spectra were performed on a Finnigan LCQ mass spectrometer. High-resolution mass spectra were performed on a Bruker 7T Apex Qe Fourier Transform Ion Cyclotron resonance mass spectrometer equipped with an Apollo II ESI/APCI/MALDI Dual source. Elemental microanalysis was obtained from the School of Human Sciences at London Metropolitan University, England. High performance liquid chromatography (HPLC) was performed on the Waters Alliance 2695 apparatus equipped with Waters 2996 photodiode array detector, set at 254 nm. HPLC data are recorded as percentage purity and retention time (RT) in minutes. Separation using a SunFire™ C18 column (5 μm, 2.1 x 150 mm) was achieved using water (solvent A) and acetonitrile (solvent B) at a flow rate of 0.2 mL/min. The method consisted of 0% B to 100% B over 30 minutes.

Carbazole Acetamide Ligands

The spectroscopic data for synthesised compounds **8–10** and **3a**, **3b** and **3d** matched previously reported data.²⁶

The spectroscopic data for synthesised compound **3c** matched previously reported data.²⁶

Pyrazolopyrimidine Acetamide Ligands

The spectroscopic data for synthesised compounds **12,13,14** matched previously reported data.²⁷

The spectroscopic data for synthesised compounds **4c** matched previously reported data.²¹

2-(2-(4-methoxyphenyl)-5,7-dimethylpyrazolo[1,5-a]pyrimidin-3-yl)acetic acid (15)

To a solution of **14** (1.52 g, 5.01 mmol, 1.0 equiv.) in ethanol (20 mL) was added acetylacetone (560 μL, 5.51 mmol, 1.1 equiv.). The reaction mixture was heated to reflux for 5 hours. Sodium hydroxide (400 mg, 10.02 mmol, 2.0 equiv.) was added, and the reaction mixture heated at reflux for a further 12 hours. The reaction mixture was cooled to ambient temperature and evaporated to dryness. The residue was then diluted in dichloromethane/isopropanol (50 mL, 1:1 v/v) and washed with aqueous hydrochloric acid (1 M, 20 mL). The organic layer was collected, dried over anhydrous magnesium sulfate and concentrated *in vacuo*. The desired product **15** was obtained as a colourless solid. Yield 92%. ¹H NMR (300 MHz, CDCl₃) δ = 12.37 (br s, 1H), 7.72 (d, *J* = 8.7 Hz, 2H), 7.07 (d, *J* = 8.7 Hz, 2H), 6.86 (s, 1H), 3.81 (s, 2H), 3.70 (s, 3H), 2.71 (s, 3H), 2.51 (s, 3H); ¹³C NMR (75 MHz, CDCl₃) δ = 172.67, 159.46, 157.75, 153.15, 147.25, 144.64, 129.08, 125.71, 114.11, 108.56,

99.22, 55.18, 28.78, 24.19, 16.25; **LRMS (-ESI)** 310 [(M - H)⁻ 100%]; Found: C, 65.63; H, 5.44; N, 13.46 Calc for C₁₇H₁₇N₃O₃: C, 65.58; H, 5.50; N, 13.50%.

General Procedure for the Synthesis of 4a–4b and 4d:

A solution of carboxylic acid intermediate **15** (100 mg, 0.321 mmol, 1.0 equiv.), appropriate secondary amine (1.1 equiv.), triethylamine (50 μ L, 0.353 mmol, 1.1 equiv) and PyBOP (180 mg, 0.353 mmol, 1.1 equiv.) in *N,N*-dimethylformamide (1 mL) was stirred at ambient temperature for 5 hours. The reaction mixture was then diluted with ethyl acetate (10 mL) and saturated aqueous ammonium chloride (10 mL). The organic layer was collected, washed with water (2 x 10 mL) and brine (1 x 10 mL). The combined organic extracts were dried over anhydrous magnesium sulfate and concentrated *in vacuo*. Unless otherwise stated, purification was achieved by flash column chromatography, followed by recrystallisation.

N-Benzyl-2-(2-(4-methoxyphenyl)-5,7-dimethylpyrazolo[1,5-*a*]pyrimidin-3-yl)-*N*-methylacetamide (**4a**)

General procedure was followed using *N*-benzylmethylamine (45 μ L, 0.353 mmol). Purification by flash chromatography (100% ethyl acetate) and recrystallisation from ethyl acetate/hexane furnished **4b** as a yellow crystals. Yield 51%. **¹H NMR (500 MHz, CDCl₃) δ = 7.80–7.75 (m, 2H), 7.31–7.21 (m, 4H), 7.13–7.11 (m, 1H), 7.00–6.96 (m, 2H), 6.51 (s, 1H), 4.62 (s, 2H), 3.99 (s, 2H), 3.85 (s, 3H), 3.05 (s, 3H), 2.74 (s, 3H), 2.54 (s, 3H); ¹³C NMR (151 MHz, CDCl₃) δ = 171.63, 159.92, 157.70, 155.16, 147.71, 144.94, 137.62, 136.83, 130.05, 128.65, 128.58, 128.15, 127.31, 127.29, 126.35, 126.25, 114.10, 108.20, 100.53, 55.39, 51.39, 35.37, 28.62, 24.73, 17.02; **LRMS (+ESI)** 437 [(M + Na)⁺ 100%], 415 [(M + H)⁺ 60%]; **HPLC** T_R = 24.61 min (98.2% purity).**

N-Benzyl-*N*-ethyl-2-(2-(4-methoxyphenyl)-5,7-dimethylpyrazolo[1,5-*a*]pyrimidin-3-yl)acetamide (**4b**)

General procedure was followed using *N*-ethylbenzylamine (50 μ L, 0.353 mmol). Purification by flash chromatography (100% ethyl acetate) and recrystallisation from ethyl acetate/ hexane furnished **4b** as a yellow solid. Yield 48%. **¹H NMR (500 MHz, CDCl₃) δ = 7.72–7.69 (m, 2H), 7.22–7.13 (m, 4H), 7.04–7.02 (m, 1H), 6.93–6.88 (m, 2H), 6.44 (s, 1H), 4.57 (s, 2H), 3.94 (s, 2H), 3.78 (s, 3H), 3.41 (q, *J* = 7.1 Hz, 2H), 2.68 (s, 3H), 2.47 (s, 3H), 1.10 (t, *J* = 7.1 Hz, 3H); ¹³C NMR (126 MHz, CDCl₃) δ = 171.23, 159.97, 157.69, 155.23, 147.86, 144.92, 138.25, 137.37, 130.13, 128.60, 128.53, 128.19, 127.21, 126.46, 126.37, 126.27, 114.15, 108.33, 100.86, 55.46, 48.52, 42.17, 28.11, 24.79, 17.07, 13.96; **LRMS (+ESI)** 451 [(M + Na)⁺ 100%], 429 [(M + H)⁺ 60%]; **HPLC** T_R = 25.86 min (97.7% purity).**

2-(2-(4-Methoxyphenyl)-5,7-dimethylpyrazolo[1,5-*a*]pyrimidin-3-yl)-*N,N*-dimethylacetamide (**4d**)

General procedure was followed using dimethylamine hydrochloride (58 mg, 0.707 mmol, 2.2 equiv.) and triethylamine (130 μ L, 0.964 mmol, 3.0 equiv.). Purification by flash chromatography (methanol/ethyl acetate 1:9 v/v) furnished **4d** as a yellow solid. Yield 80%. **¹H NMR (300 MHz, CDCl₃) δ = 7.75 (d, *J* = 8.2 Hz, 2H), 6.98 (d, *J* = 8.2 Hz, 2H), 6.49 (s, 1H), 3.91 (s, 2H), 3.84 (s, 3H), 3.15 (s, 3H), 2.97 (s, 3H), 2.72 (s, 3H), 2.52 (s, 3H); ¹³C NMR (75 MHz, CDCl₃) δ = 171.17, 159.91, 157.64, 155.17, 147.67, 144.88, 130.03, 126.35, 114.12, 108.32, 100.47, 55.41, 37.78, 36.04, 28.48, 24.76, 17.01; **LRMS (+ESI)** 361 [(M + Na)⁺ 100%], 339 [(M + H)⁺ 50%]; **HPLC** T_R = 19.71 min (96.7% purity).**

Pyrazolobenzodiazepine Acetamide Ligands

General Procedure for the Synthesis of 5a–5d:

To a solution of **16** (100 mg, 0.499 mmol, 1.0 equiv.) in tetrahydrofuran (1 mL) was added triethylamine (140 μ L, 0.999 mmol, 2.0 equiv.), followed by the dropwise addition of the appropriate

alkylating agent (1.1 equiv.). The reaction mixture was stirred at ambient temperature for 19 hours. The reaction mixture was evaporated to dryness and diluted with ethyl acetate (5 mL) and water (2 mL). The organic layer was collected, and the aqueous layer was further extracted with ethyl acetate (2 x 5 mL). The combined organic extracts were washed with aqueous hydrochloric acid (1 M, 2 mL), followed by water (2 mL). The organic layer was dried over magnesium sulfate and concentrated *in vacuo*. Purification by flash chromatography on silica gel column using methanol/dichloromethane (5:95 v/v) furnished the desired pyrazolobenzodiazepine ligands.

N-Benzyl-*N*-methyl-2-(1-methyl-4,10-dihydrobenzo[*b*]pyrazolo[3,4-*e*][1,4]diazepin-5(1*H*)-yl)acetamide (**5a**)

General procedure was followed using alkylating agent *N*-benzyl-2-bromo-*N*-methylacetamide (133 mg, 0.549 mmol). The desired product **5a** was isolated as a beige powder. Yield 85%. **¹H NMR (300 MHz, CDCl₃)** δ = 7.28–7.25 (m, 3H), 7.14–6.87 (m, 7H), 5.90 (s, 1H), 4.59 (s, 2H), 4.04 (s, 2H), 3.88 (s, 2H), 3.70 (s, 3H), 2.98 (s, 3H); **¹³C NMR (75 MHz, CDCl₃)** δ = 169.81, 140.24, 138.74, 137.36, 136.63, 130.88, 128.69, 128.42, 128.03, 126.41, 125.84, 122.44, 119.26, 101.19, 57.09, 50.75, 47.75, 38.22, 34.36; **LRMS (+ESI)** 384 ([M + Na]⁺ 100%); Found: C, 69.83; H, 6.47; N, 19.36. Calc for C₂₁H₂₃N₅O: C, 69.78; H, 6.41; N, 19.38%.

N-Benzyl-*N*-ethyl-2-(1-methyl-4,10-dihydrobenzo[*b*]pyrazolo[3,4-*e*][1,4]diazepin-5(1*H*)-yl)acetamide (**5b**)

General procedure was followed using alkylating agent *N*-benzyl-2-bromo-*N*-ethylacetamide (141 mg, 0.549 mmol). The desired product **5b** was isolated as a beige powder. Yield 83%. **R_f** 0.63 (methanol/dichloromethane, 1:9 v/v); **¹H NMR (300 MHz, CDCl₃)** δ = 7.29–7.21 (m, 3H), 7.14–6.81 (m, 7H), 5.90 (s, 1H), 4.62 (s, 2H), 4.12 (s, 2H), 3.92 (s, 2H), 3.70 (s, 3H), 3.36 (t, *J* = 7.1 Hz, 2H), 1.07 (q, *J* = 7.1 Hz, 3H); **¹³C NMR (75 MHz, CDCl₃)** δ = 170.82, 141.16, 140.22, 138.88, 137.25, 135.96, 128.20, 128.02, 127.14, 126.34, 125.35, 121.47, 119.32, 100.89, 56.02, 50.04, 47.59, 41.49, 34.98, 13.81; **LRMS (+ESI)** 398 ([M + Na]⁺ 100%); Found: C, 70.26; H, 6.69; N, 18.71. Calc for C₂₂H₂₅N₅O: C, 70.38; H, 6.71; N, 18.65%.

N,N-Diethyl-2-(1-methyl-4,10-dihydrobenzo[*b*]pyrazolo[3,4-*e*][1,4]diazepin-5(1*H*)-yl)acetamide (**5c**)

General procedure was followed using alkylating agent 2-chloro-*N,N*-diethylacetamide (75 μ L, 0.549 mmol). The desired product **5c** was isolated as a beige powder. Yield 86%. **¹H NMR (300 MHz, CDCl₃)** δ = 7.24 (s, 1H), 6.92–6.70 (m, 4H), 6.03 (s, 1H), 4.69 (s, 2H), 3.97 (s, 2H), 3.63 (s, 3H), 3.34 (q, *J* = 7.4 Hz, 4H), 1.03 (t, *J* = 7.4 Hz, 6H); **¹³C NMR (75 MHz, CDCl₃)** δ = 168.90, 142.07, 138.57, 137.66, 131.36, 126.80, 125.09, 122.58, 118.85, 101.17, 56.90, 50.16, 41.20, 40.66, 34.66, 13.61, 12.33; **LRMS (+ESI)** 336 ([M + Na]⁺ 60%), 314 ([M + H]⁺ 100%); Found: C, 65.11; H, 7.33; N, 22.38. Calc for C₁₇H₂₃N₅O: C, 65.15; H, 7.40; N, 22.35%.

N,N-Dimethyl-2-(1-methyl-4,10-dihydrobenzo[*b*]pyrazolo[3,4-*e*][1,4]diazepin-5(1*H*)-yl)acetamide (**5d**)

General procedure was followed using alkylating agent 2-chloro-*N,N*-dimethylacetamide (70 mg, 0.549 mmol). The desired product **5d** was isolated as a colourless powder. Yield 83%. **¹H NMR (300 MHz, CDCl₃)** δ = 7.26 (s, 1H), 6.91–6.71 (m, 4H), 5.83 (s, 1H), 4.61 (s, 2H), 3.90 (s, 2H), 3.68 (s, 3H), 3.01 (s, 6H); **¹³C NMR (75 MHz, CDCl₃)** δ = 169.85, 140.23, 138.43, 137.12, 131.41, 126.57, 125.22, 122.26, 119.30, 101.26, 57.14, 50.39, 36.71, 36.12, 34.59. **LRMS (+ESI)** 308 ([M + Na]⁺ 50%), 286 ([M + H]⁺ 100%); Found: C, 63.09; H, 6.68; N, 24.60. Calc for C₁₅H₁₉N₅O: C, 63.14; H, 6.71; N, 24.54.

Dibenzodiazepine Acetamide Ligands

Methyl 2-((2-nitrophenyl)amino)benzoate (19)

A suspension of 2-iodonitrobenzene (**17**) (1.00 g, 4.02 mmol, 1.0 equiv.), methyl anthranilate (**18**) (520 μ L, 4.02 mmol, 1.0 equiv.), BINAP (250 mg, 0.402 mmol, 10 mol%) and caesium carbonate (2.62 g, 8.03 mmol, 2.0 equiv.) in toluene (20 mL) was degassed with argon sparging for 10 minutes. Palladium acetate (45 mg, 0.201 mmol, 5 mol%) was added under argon. The reaction mixture was stirred at 80 °C for 18 hours. The reaction mixture was cooled to ambient temperature and evaporated to dryness. The crude material was diluted with ethyl acetate and filtered through a pad of Celite®. The pad of Celite® was washed with ethyl acetate and the combined filtrates concentrated *in vacuo*. Purification by flash column chromatography on silica gel using ethyl acetate/hexane (1:9 v/v) furnished **19** as an orange powder. Yield 77%. **¹H NMR (400 MHz, CDCl₃)** δ = 11.13 (br s, 1H), 8.19 (dd, *J* = 8.4, 1.6 Hz, 1H), 8.06 (dd, *J* = 7.9, 1.7 Hz, 1H), 7.67–7.57 (m, 1H), 7.55–7.49 (m, 1H), 7.46 (ddt, *J* = 8.6, 7.0, 1.7 Hz, 2H), 7.11–7.01 (m, 1H), 6.96 (ddt, *J* = 8.3, 7.0, 1.1 Hz, 1H), 3.99 (s, 3H); **¹³C NMR (101 MHz, CDCl₃)** δ = 167.46, 142.30, 139.08, 137.39, 134.65, 133.37, 132.05, 126.64, 121.81, 119.89, 119.03, 118.71, 118.59, 52.30; **LRMS (+ESI)** 295 [(M + Na)⁺ 100%].

Methyl 2-((2-aminophenyl)amino)benzoate (20)

To a mixture of **19** (600 mg, 2.20 mmol, 1.0 equiv.) in ethyl acetate (20 mL) was added palladium on carbon (60 mg, 10% w/w). The reaction mixture was stirred at ambient temperature for 18 hours under a hydrogen atmosphere (1 atm). The reaction mixture was filtered through a pad of Celite® and the pad was washed with ethyl acetate. The combined filtrates were evaporated *in vacuo*. Purification by flash column chromatography on silica gel using ethyl acetate/hexane (1:9 v/v) furnished **20** as a colourless powder. Yield 92%. **¹H NMR (400 MHz, CDCl₃)** δ = 8.98 (br s, 1H), 7.98 (dd, *J* = 8.1, 1.7 Hz, 1H), 7.32–7.27 (m, 1H), 7.17–7.09 (m, 2H), 6.85–6.76 (m, 2H), 6.73–6.65 (m, 2H), 3.94 (s, 3H), 3.84 (br s, 2H); **¹³C NMR (101 MHz, CDCl₃)** δ = 169.07, 149.54, 143.38, 134.39, 131.41, 127.76, 127.14, 125.93, 118.80, 116.38, 115.92, 113.79, 111.01, 52.30; **LRMS (+ESI)** 265 [(M + Na)⁺ 100%].

5,10-Dihydro-11H-dibenzo[b,e][1,4]diazepin-11-one (21)

A suspension of **20** (400 mg, 1.65 mmol, 1.0 equiv.) and lithium hydroxide (158 mg, 6.60 mmol, 4.0 equiv.) in methanol/water (10 mL, 1:1 v/v) was stirred at reflux for 6 hours. The reaction mixture was then cooled and the methanol evaporated under reduced pressure. The mixture was diluted with ethyl acetate (20 mL) and acidified using aqueous hydrochloric acid (1 M, 20 mL). The organic layer was collected and the aqueous layer further extracted with ethyl acetate (2 x 10 mL). The combined organic extracts were then dried and evaporated *in vacuo* to give the desired crude carboxylic acid intermediate. The crude material was carried onto the next step without purification.

A solution of the crude carboxylic intermediate, HBTU (922 mg, 2.43 mmol, 1.5 equiv.) and *N,N*-diisopropylethylamine (560 μ L, 3.24 mmol, 2.0 equiv.) in *N,N*-dimethylformamide (5 mL) was stirred at ambient temperature for 5 minutes. The reaction mixture was then poured into ice-cold water (5 mL) and diluted with ethyl acetate (20 mL). The organic layer was extracted and the aqueous layer further extracted with ethyl acetate (2 x 10 mL). The combined organic extracts were then washed with aqueous hydrochloric acid (1 M, 10 mL), an aqueous solution of saturated sodium bicarbonate (10 mL) and water (10 mL). The organic extract was then dried over magnesium sulfate and evaporated *in vacuo*. Purification by flash column chromatography on silica gel using ethyl acetate/hexane (3:7 v/v) furnished **21** as a yellow powder. Yield 82%. **¹H NMR (400 MHz, DMSO)** δ = 9.83 (br s, 1H), 7.84 (br s, 1H), 7.68 (dd, *J* = 7.9, 1.7 Hz, 1H), 7.34 (ddd, *J* = 8.1, 7.1, 1.7 Hz, 1H), 7.07–6.82 (m, 6H); **¹³C NMR (101 MHz, DMSO)** δ = 168.38, 150.91, 140.42, 133.66, 132.56, 130.29, 124.95, 123.40, 123.23, 121.73, 121.16, 120.23, 119.52; **LRMS (+ESI)** 233 [(M + Na)⁺ 100%].

General Procedure for the Synthesis of 6a–6d

To a solution of **21** (50 mg, 0.238 mmol, 1.0 equiv.) in tetrahydrofuran (0.2 M) was added potassium *tert*-butoxide (40 mg, 0.357 mmol, 1.5 equiv.) at 0 °C and stirred for 30 minutes at ambient temperature. The reaction mixture was cooled to 0 °C and the appropriate alkylating agent (1.1 equiv.) was added dropwise. The reaction mixture was warmed to ambient temperature and stirred for 8 hours. The reaction mixture was quenched with water at 0 °C and then diluted with ethyl acetate (10 mL). The organic layer was collected and the aqueous layer was further extracted with ethyl acetate (2 x 5 mL). The combined organic extracts were then washed with brine (2 mL), dried over magnesium sulfate and concentrated *in vacuo*. Purification by flash chromatography on silica gel column using ethyl acetate/hexane (1:1 v/v) furnished the desired dibenzodiazepine ligands.

N-Benzyl-*N*-methyl-2-(11-oxo-10,11-dihydro-5H-dibenzo[*b,e*][1,4]diazepin-5-yl)acetamide (**6a**)

General procedure was followed using alkylating agent, *N*-benzyl-2-bromo-*N*-methylacetamide (63 mg, 0.262 mmol). The desired product **6a** was isolated as a colourless powder. Yield 86%. **¹H NMR (400 MHz, CDCl₃)** δ = 7.91 (dd, *J* = 7.8, 1.6 Hz, 1H), 7.45–7.25 (m, 7H), 7.12–7.04 (m, 3H) 6.94–6.92 (m, 1H), 6.82–6.79 (m, 1H), 5.37 (br s, 1H), 4.80 (s, 2H), 4.70 (s, 2H), 3.05 (s, 3H); **¹³C NMR (101 MHz, CDCl₃)** δ = 173.20, 170.37, 150.51, 141.67, 137.01, 134.60, 133.10, 132.55, 128.63, 128.02, 127.35, 126.50, 124.53, 123.37, 122.73, 120.19, 120.05, 118.46, 52.82, 51.44, 34.37; **LRMS (+ESI)** 394 [(M + Na)⁺ 100%]; Found: C, 74.29; H, 5.69; N, 11.26. Calc for C₂₃H₂₁N₃O₂: C, 74.37; H, 5.70; N, 11.31.

N-Benzyl-*N*-ethyl-2-(11-oxo-10,11-dihydro-5H-dibenzo[*b,e*][1,4]diazepin-5-yl)acetamide (**6b**)

General procedure was followed using alkylating agent, *N*-benzyl-2-bromo-*N*-ethylacetamide (67 mg, 0.262 mmol). The desired product **6b** was isolated as a colourless powder. Yield 92%. **¹H NMR (400 MHz, DMSO)** δ = 7.88 (dd, *J* = 9.4, 1.6 Hz, 1H), 7.63–7.60 (m, 1H), 7.42–7.25 (m, 6H), 7.14–6.95 (m, 4H), 6.99–6.65 (m, 1H), 4.73 (s, 2H), 4.61 (s, 2H), 3.36 (q, *J* = 7.1 Hz, 2H), 1.17 (t, *J* = 7.1 Hz, 3H), *NH* proton not observed; **¹³C NMR (101 MHz, DMSO)** δ = 168.12, 167.66, 152.34, 144.42, 138.61, 135.07, 132.96, 132.56, 128.85, 127.90, 127.30, 126.02, 124.67, 123.90, 123.76, 121.82, 120.65, 119.25 52.96, 48.15, 41.10, 14.01; **LRMS (+ESI)** 408 [(M + Na)⁺ 100%]; Found: C, 74.79; H, 6.03; N, 10.94. Calc for C₂₄H₂₃N₃O₂: C, 74.78; H, 6.01; N, 10.90.

N,N-Diethyl-2-(11-oxo-10,11-dihydro-5H-dibenzo[*b,e*][1,4]diazepin-5-yl)acetamide (**6c**)

General procedure was followed using alkylating agent, 2-chloro-*N,N*-diethylacetamide (35 μL, 0.262 mmol). The desired product **6c** was isolated as a colourless powder. Yield 83%. **¹H NMR (400 MHz, DMSO)** δ = 7.86 (br s, 1H), 7.58 (dd, *J* = 7.8, 1.6 Hz, 1H), 7.34 (ddd, *J* = 8.5, 7.2, 1.7 Hz, 1H), 7.18 (dd, *J* = 7.7, 1.7 Hz, 1H) 7.14–6.92 (m, 5H), 4.58 (s, 2H), 3.38 (t, *J* = 7.1 Hz, 4H), 1.20 (q, *J* = 7.1 Hz, 3H), 1.08 (q, *J* = 7.1 Hz, 3H); **¹³C NMR (101 MHz, DMSO)** δ = 168.01, 167.02, 152.29, 144.36, 135.14, 132.88, 132.51, 125.95, 124.79, 123.86, 123.69, 121.79, 120.58, 119.21 53.16, 41.13, 13.54; **LRMS (+ESI)** 346 [(M + Na)⁺ 100%]; Found: C, 70.51; H, 6.49; N, 12.93. Calc for C₁₉H₂₁N₃O₂: C, 70.57; H, 6.55; N, 12.99.

N,N-Dimethyl-2-(11-oxo-10,11-dihydro-5H-dibenzo[*b,e*][1,4]diazepin-5-yl)acetamide (**6d**)

General procedure was followed using alkylating agent, 2-chloro-*N,N*-dimethylacetamide (25 μL, 0.262 mmol). The desired product **6d** was isolated as a colourless powder. Yield 75%. **¹H NMR (400 MHz, DMSO)** δ = 7.87 (br s, 1H), 7.52 (dd, *J* = 7.8, 1.6 Hz, 1H), 7.37–7.31 (m, 1H), 7.19 (d, *J* = 7.8 Hz, 1H), 7.18–6.91 (m, 5H), 4.58 (s, 2H), 3.11 (s, 6H); **¹³C NMR (101 MHz, DMSO)** δ = 168.08, 166.98, 151.84, 144.31, 136.01, 132.74, 132.50, 126.19, 124.84, 123.89, 123.79, 122.52, 120.56, 119.22 52.95, 36.69, 36.11; **LRMS (+ESI)** 318 [(M + Na)⁺ 100%]; Found: C, 69.18; H, 5.86; N, 14.19. Calc for C₁₇H₁₇N₃O₂: C, 69.14; H, 5.80; N, 14.23.

Biological Evaluation

Radioligand binding. Binding affinities (K_i) to wild type and A147T TSPO were measured as per our published protocol.²⁰ Briefly, membranes were prepared from HEK293T cells stably transfected with wild type and A147T TSPO by homogenisation, using an Ultra-Turrax hand-held homogeniser. These cells have previously been validated as an *in vitro* model of low- and high- affinity TSPO binders.²⁰ Wild type (20 $\mu\text{g}/\text{well}$) and A147T (5 $\mu\text{g}/\text{well}$) TSPO membranes were diluted in 50 mM Tris HCl (pH 7.4), and were incubated at 4 °C for 90 min with $\sim K_i$ concentration of [³H] PK 11195 (10 nM; Perkin Elmer) and test compounds (0.3 nM–10 μM). A high concentration (1 μM) of unlabelled PK 11195 was used to measure non-specific binding, which was less than 10% of total binding. Filtration through a 96-well glass-fibre filter plate (Millipore) was used to terminate reactions. Plates were then washed 8 times with ice-cold 50 mM Tris HCl. Radioactivity was read in a Microbeta² 2450 Microplate Counter (Perkin Elmer) after addition of Microscint 0. Data were analysed using Graphpad Prism 6.0 (GraphPad), applying a four-parameter non-linear regression curve fit to calculate K_i values. Data are expressed as mean \pm SEM from at least three independent experiments.

Target protein preparation. The WT and A147T TSPO homology models generated in our previous study,²⁰ were prepared using preparation and refinement protocols, directed by the Protein Preparation Wizard²⁸ embedded in Maestro v12.1 (Schrödinger, LLC, New York, USA). This process includes assigning bond orders, adding hydrogen atoms, and creating zero order bonds to metals and disulphide bonds. The hydrogen bond network within the protein was also optimised with all het groups within the receptor grid bounding box previously removed and the protein structure minimised to a root mean square deviation (RMSD) of 0.3 Å using the OPLS3 force field.^{29, 30}

Ligand preparation. All ligands were prepared using the LigPrep v4.9 module to generate possible stereoisomers of the ligands as well as generating all potential ionisation states at pH 7 \pm 2. Confgen³¹ v4.7 was also used to generate up to 64 different conformations for each ligand.

Receptor grid generation. The Receptor Grid Generation tool in Glide v8.4^{32, 33} as used to characterise the binding site for the docking studies. Binding sites were defined by a 20 Å³ bounding box centred at the ligand within the active site of each homology model. A Coulomb-van der Waals scaling factor of 1.0 for receptor van der Waals radii was applied to protein atoms with a partial charge of less than 0.25 e and a similar factor of 0.8 was applied to ligand atoms with a partial charge cutoff of less than 0.15 e. Rotations of hydroxyl and thiol groups were not allowed.

Docking studies. The ligands were docked into the receptor grids with Glide v8.4.^{32, 33} All docking studies were carried out using the Extra Precision (XP)³⁴ scoring function to refine binding energy estimates. All ligands were docked with flexible states to allow sampling of the effect of nitrogen inversion, changing ring conformations and non-planar amide functional groups were penalised. Prime MM-GBSA calculations,³⁵ which combines molecular mechanics (MM) terms, and a generalised Born and surface area (GBSA) solvent model,²⁵ were utilised to calculate the free energy of binding for the ligands. The output poses from Glide XP docking were used as the basis for these calculations. The calculations were performed using the variable-dielectric generalised Born (VSGB)³⁶ solvation model and OPLS3 force field.³⁰ The docked ligand and protein residues within 10 Å of the ligand were allowed to be flexible, with all other atoms remaining rigid.

Author Contributions:

R.S. and E.L.W. are co-first-authors[§], contributing equally to this work, carrying out synthesis and affinity measurements, respectively. H.W.A.C assisted with the pharmacological screening while J.H.L., J.J.D., G.S., T.A.R. and M.K. assisted with the design and synthesis of ligands. The transfected HEK293 cells were provided by L.M.I. A.P.M., J.J.D., Q.G. and D.E.H. provided the TSPO docking studies for ligands **3a**, **4a**, **5a** and **6a**. All authors contributed to the writing and proof-reading of the manuscript.

Corresponding Author

* M.K. Telephone: +61 2 9351 2745. Fax: +61 2 9351 3329. Email: michael.kassiou@sydney.edu.au

Funding Sources

The work was supported by the National Health and Medical Research Council of Australia (APP1132524, 1136241 and 1154692).

ACKNOWLEDGEMENT

The authors wish to also thank Dr Sheng Hua and Dr Donna Lai for assistance with the Bosch Molecular Biology Facility.

ABBREVIATIONS USED

AcOH, acetic acid; MeCN, acetonitrile; PyBOP, benzotriazol-1-yl-oxytripyrrolidinophosphonium hexafluorophosphate; BINAP, 2,2'-bis(diphenylphosphino)-1,1'-binaphthalene; Cs₂CO₃, caesium carbonate; d, doublet; DIPEA, diisopropylethylamine; DMF, dimethylformamide; EtOH, ethanol; EtOAc, ethyl acetate; h, hours; HEK, human embryonic kidney; HPLC, high-performance liquid chromatography; H₂, hydrogen gas; K_i, inhibitor constant; kDa, kilodalton; LiOH, lithium hydroxide; MeOH, methanol; μM, micromolar; nM, nanomolar; HBTU, *N,N,N',N'*-tetramethyl-*O*-(1H-benzotriazol-1-yl)uronium hexafluorophosphate; Pd(OAc)₂, palladium acetate; Pd/C, palladium on carbon; PET, positron emission tomography; KOtBu, potassium *tert*-butoxide; rt, room temperature; s, singlet; NaOH, sodium hydroxide; NaH, sodium hydride; NaOMe, sodium methoxide; SD, standard deviation; SAR, structure-activity relationship; Pd(PPh₃)₄, tetrakis(triphenylphosphine)palladium(0); t, triplet; THF, tetrahydrofuran; PhMe, toluene; TSPO, translocator protein; Et₃N, triethylamine.

References

1. Papadopoulos, V.; Baraldi, M.; Guilarte, T. R.; Knudsen, T. B.; Lacapere, J. J.; Lindemann, P.; Norenberg, M. D.; Nutt, D.; Weizman, A.; Zhang, M. R.; Gavish, M., Translocator protein (18kDa): new nomenclature for the peripheral-type benzodiazepine receptor based on its structure and molecular function. *Trends Pharmacol Sci* **2006**, *27*(8), 402-409.
2. Chen, M. K.; Guilarte, T. R., Translocator protein 18 kDa (TSPO): molecular sensor of brain injury and repair. *Pharmacol Ther* **2008**, *118*(1), 1-17.
3. Gavish, M.; Bachman, I.; Shoukrun, R.; Katz, Y.; Veenman, L.; Weisinger, G.; Weizman, A., Enigma of the peripheral benzodiazepine receptor. *Pharmacol Rev* **1999**, *51*(4), 629-650.
4. Owen, D. R.; Matthews, P. M., Imaging brain microglial activation using positron emission tomography and translocator protein-specific radioligands. *Int Rev Neurobiol* **2011**, *101*, 19-39.
5. Werry, E. L.; Barron, M. L.; Kassiou, M., TSPO as a target for glioblastoma therapeutics. *Biochem Soc Trans* **2015**, *43*(4), 531-536.
6. Roncaroli, F.; Su, Z.; Herholz, K.; Gerhard, A.; Turkheimer, F. E., TSPO expression in brain tumours: is TSPO a target for brain tumour imaging? *Clin Transl Imaging* **2016**, *4*, 145-156.

7. Owen, D. R.; Yeo, A. J.; Gunn, R. N.; Song, K.; Wadsworth, G.; Lewis, A.; Rhodes, C.; Pulford, D. J.; Bennacef, I.; Parker, C. A.; StJean, P. L.; Cardon, L. R.; Mooser, V. E.; Matthews, P. M.; Rabiner, E. A.; Rubio, J. P., An 18-kDa translocator protein (TSPO) polymorphism explains differences in binding affinity of the PET radioligand PBR28. *J Cereb Blood Flow Metab* **2012**, *32* (1), 1-5.
8. Owen, D. R.; Gunn, R. N.; Rabiner, E. A.; Bennacef, I.; Fujita, M.; Kreisl, W. C.; Innis, R. B.; Pike, V. W.; Reynolds, R.; Matthews, P. M.; Parker, C. A., Mixed-affinity binding in humans with 18-kDa translocator protein ligands. *J Nucl Med* **2011**, *52* (1), 24-32.
9. Owen, D. R.; Lewis, A. J.; Reynolds, R.; Rupprecht, R.; Eser, D.; Wilkins, M. R.; Bennacef, I.; Nutt, D. J.; Parker, C. A., Variation in binding affinity of the novel anxiolytic XBD173 for the 18 kDa translocator protein in human brain. *Synapse* **2011**, *65* (3), 257-259.
10. Zanotti-Fregonara, P.; Zhang, Y.; Jenko, K. J.; Gladding, R. L.; Zoghbi, S. S.; Fujita, M.; Sbardella, G.; Castellano, S.; Taliani, S.; Martini, C.; Innis, R. B.; Da Settimo, F.; Pike, V. W., Synthesis and evaluation of translocator 18 kDa protein (TSPO) positron emission tomography (PET) radioligands with low binding sensitivity to human single nucleotide polymorphism rs6971. *ACS Chem Neurosci* **2014**, *5* (10), 963-971.
11. Vivash, L.; O'Brien, T. J., Imaging Microglial Activation with TSPO PET: Lighting Up Neurologic Diseases? *J Nucl Med* **2016**, *57* (2), 165-168.
12. Chauveau, F.; Boutin, H.; Van Camp, N.; Dolle, F.; Tavitian, B., Nuclear imaging of neuroinflammation: a comprehensive review of [¹¹C]PK11195 challengers. *Eur J Nucl Med Mol Imaging* **2008**, *35* (12), 2304-2319.
13. Ikawa, M.; Lohith, T. G.; Shrestha, S.; Telu, S.; Zoghbi, S. S.; Castellano, S.; Taliani, S.; Da Settimo, F.; Fujita, M.; Pike, V. W.; Innis, R. B.; Biomarkers Consortium Radioligand Project, T., ¹¹C-ER176, a Radioligand for 18-kDa Translocator Protein, Has Adequate Sensitivity to Robustly Image All Three Affinity Genotypes in Human Brain. *J Nucl Med* **2017**, *58* (2), 320-325.
14. Taliani, S.; Pugliesi, I.; Da Settimo, F., Structural requirements to obtain highly potent and selective 18 kDa Translocator Protein (TSPO) Ligands. *Curr Top Med Chem* **2011**, *11* (7), 860-886.
15. Kim, T.; Pae, A. N., Translocator protein (TSPO) ligands for the diagnosis or treatment of neurodegenerative diseases: a patent review (2010-2015; part 1). *Expert Opin Ther Pat* **2016**, *26* (11), 1325-1351.
16. Matarrese, M.; Moresco, R. M.; Cappelli, A.; Anzini, M.; Vomero, S.; Simonelli, P.; Verza, E.; Magni, F.; Sudati, F.; Soloviev, D.; Todde, S.; Carpinelli, A.; Kienle, M. G.; Fazio, F., Labeling and evaluation of N-[¹¹C]methylated quinoline-2-carboxamides as potential radioligands for visualization of peripheral benzodiazepine receptors. *J Med Chem* **2001**, *44* (4), 579-585.
17. Sherer, C.; Snape, T. J., Heterocyclic scaffolds as promising anticancer agents against tumours of the central nervous system: Exploring the scope of indole and carbazole derivatives. *Eur J Med Chem* **2015**, *97*, 552-560.
18. Welsch, M. E.; Snyder, S. A.; Stockwell, B. R., Privileged scaffolds for library design and drug discovery. *Curr Opin Chem Biol* **2010**, *14* (3), 347-361.
19. Kombarov, R.; Altieri, A.; Genis, D.; Kirpichenok, M.; Kochubey, V.; Rakitina, N.; Titarenko, Z., BioCores: identification of a drug/natural product-based privileged structural motif for small-molecule lead discovery. *Mol Divers* **2010**, *14* (1), 193-200.
20. Cheng, H. W. A.; Sokias, R.; Werry, E. L.; Ittner, L. M.; Reekie, T. A.; Du, J.; Gao, Q.; Hibbs, D. E.; Kassiou, M., First Nondiscriminating Translocator Protein Ligands Produced from a Carbazole Scaffold. *J Med Chem* **2019**, *62* (17), 8235-8248.
21. Reynolds, A.; Hanani, R.; Hibbs, D.; Damont, A.; Da Pozzo, E.; Selleri, S.; Dolle, F.; Martini, C.; Kassiou, M., Pyrazolo[1,5-a]pyrimidine acetamides: 4-Phenyl alkyl ether derivatives as potent ligands for the 18 kDa translocator protein (TSPO). *Bioorg Med Chem Lett* **2010**, *20* (19), 5799-5802.
22. Katte, T. A.; Reekie, T. A.; Jorgensen, W. T.; Kassiou, M., The Formation of Seven-Membered Heterocycles under Mild Pictet-Spengler Conditions: A Route to Pyrazolo[3,4]benzodiazepines. *J Org Chem* **2016**, *81* (11), 4883-4889.
23. Campiani, G.; Nacci, V.; Fiorini, I.; De Filippis, M. P.; Garofalo, A.; Ciani, S. M.; Greco, G.; Novellino, E.; Williams, D. C.; Zisterer, D. M.; Woods, M. J.; Mihai, C.; Manzoni, C.; Mennini, T., Synthesis, biological activity, and SARs of pyrrolobenzoxazepine derivatives, a new class of

- specific "peripheral-type" benzodiazepine receptor ligands. *J Med Chem* **1996**, *39* (18), 3435-3450.
24. Castellano, S.; Taliani, S.; Milite, C.; Pugliesi, I.; Da Pozzo, E.; Rizzetto, E.; Bendinelli, S.; Costa, B.; Cosconati, S.; Greco, G.; Novellino, E.; Sbardella, G.; Stefancich, G.; Martini, C.; Da Settimo, F., Synthesis and biological evaluation of 4-phenylquinazoline-2-carboxamides designed as a novel class of potent ligands of the translocator protein. *J Med Chem* **2012**, *55* (9), 4506-4510.
 25. Lyne, P. D.; Lamb, M. L.; Saeh, J. C., Accurate prediction of the relative potencies of members of a series of kinase inhibitors using molecular docking and MM-GBSA scoring. *J Med Chem* **2006**, *49* (16), 4805-4808.
 26. Sokias, R.; Werry, E. L.; Chua, S. W.; Reekie, T. A.; Munoz, L.; Wong, E. C. N.; Ittner, L. M.; Kassiou, M., Determination and reduction of translocator protein (TSPO) ligand rs6971 discrimination. *Medchemcomm* **2017**, *8* (1), 202-210.
 27. Li, J.; Schulte, M. L.; Nickels, M. L.; Manning, H. C., New structure-activity relationships of N-acetamide substituted pyrazolopyrimidines as pharmacological ligands of TSPO. *Bioorg Med Chem Lett* **2016**, *26* (15), 3472-7.
 28. Sastry, G. M.; Adzhigirey, M.; Day, T.; Annabhimoju, R.; Sherman, W., Protein and ligand preparation: parameters, protocols, and influence on virtual screening enrichments. *Journal of computer-aided molecular design* **2013**, *27* (3), 221-234.
 29. Sastry, G. M.; Adzhigirey, M.; Day, T.; Annabhimoju, R.; Sherman, W., Protein and ligand preparation: parameters, protocols, and influence on virtual screening enrichments. *J Comput Aided Mol Des* **2013**, *27* (3), 221-34.
 30. Harder, E.; Damm, W.; Maple, J.; Wu, C.; Reboul, M.; Xiang, J. Y.; Wang, L.; Lupyan, D.; Dahlgren, M. K.; Knight, J. L.; Kaus, J. W.; Cerutti, D. S.; Krilov, G.; Jorgensen, W. L.; Abel, R.; Friesner, R. A., OPLS3: A Force Field Providing Broad Coverage of Drug-like Small Molecules and Proteins. *J Chem Theory Comput* **2016**, *12* (1), 281-96.
 31. Watts, K. S.; Dalal, P.; Murphy, R. B.; Sherman, W.; Friesner, R. A.; Shelley, J. C., ConfGen: a conformational search method for efficient generation of bioactive conformers. *Journal of chemical information and modeling* **2010**, *50* (4), 534-546.
 32. Friesner, R. A.; Banks, J. L.; Murphy, R. B.; Halgren, T. A.; Klicic, J. J.; Mainz, D. T.; Repasky, M. P.; Knoll, E. H.; Shelley, M.; Perry, J. K.; Shaw, D. E.; Francis, P.; Shenkin, P. S., Glide: a new approach for rapid, accurate docking and scoring. 1. Method and assessment of docking accuracy. *J Med Chem* **2004**, *47* (7), 1739-49.
 33. Halgren, T. A.; Murphy, R. B.; Friesner, R. A.; Beard, H. S.; Frye, L. L.; Pollard, W. T.; Banks, J. L., Glide: a new approach for rapid, accurate docking and scoring. 2. Enrichment factors in database screening. *J Med Chem* **2004**, *47* (7), 1750-9.
 34. Friesner, R. A.; Murphy, R. B.; Repasky, M. P.; Frye, L. L.; Greenwood, J. R.; Halgren, T. A.; Sanschagrín, P. C.; Mainz, D. T., Extra precision glide: docking and scoring incorporating a model of hydrophobic enclosure for protein-ligand complexes. *J Med Chem* **2006**, *49* (21), 6177-96.
 35. Jacobson, M. P.; Friesner, R. A.; Xiang, Z.; Honig, B., On the role of the crystal environment in determining protein side-chain conformations. *J Mol Biol* **2002**, *320* (3), 597-608.
 36. Li, J.; Abel, R.; Zhu, K.; Cao, Y.; Zhao, S.; Friesner, R. A., The VSGB 2.0 model: a next generation energy model for high resolution protein structure modeling. *Proteins* **2011**, *79* (10), 2794-812.

Highlights:

- Optimal binding to both TSPO isoforms is dependent on both the heterocyclic scaffold and substituents on the acetamide motif.
- The nature of the pyrazolopyrimidine scaffold was found to be a promising scaffold for TSPO ligands.
- Lowered discrimination at A147T TSPO is predominantly seen with *N*-benzyl-*N*-methyl ligands.
- Docking studies were used to examine how each heterocyclic scaffold binds to both WT and A147T TSPO.

Journal Pre-proof

Declaration of interests

The authors declare that they have no known competing financial interests or personal relationships that could have appeared to influence the work reported in this paper.

The authors declare the following financial interests/personal relationships which may be considered as potential competing interests:

Journal Pre-proof